EUROPEAN ORGANIZATION FOR NUCLEAR RESEARCH

Proposal to the ISOLDE and Neutron Time-of-Flight Committee
(Following ISOLDE Letter of Intent I-126)

Reaction mechanisms in collisions induced by ^{8}B beam close to the barrier.

A.Di Pietro[1], P. Figuera[1], J. Ballof[2], A.Bonaccorso[3], J. Cederkall[4], T. Davinson[5], J. Fernandez-Garcia[1,6], M. Fisichella[1], M.J. Garcia-Borge[2,7], J. Gomez-Camacho[8], A. Knyazev[4], M. Lattuada[1,6], M. Madurga[2], I. Martel[9], M. Milin[10], A.M. Moro[8], D. Santonocito[1], C. Seiffert[2], A.C. Shotter[5], J. Snall[4], N. Soic[11], O. Tengbald[7], D. Torresi[1,6], M. Zadro[11]

1) INFN-Laboratori Nazionali del Sud, Catania, Italy
2) ISOLDE, CERN, Geneva, Swizerland
3) INFN-Sezione di Pisa, Pisa, Italy
4) University of Lund, Lund, Sweden
5) School of Physics, University of Edinburgh, Edinburg, UK.
6) Dipartimento di Fisica e Astronomia, Universita' di Catania, Catania, Italy
7) Instituto de Estructura de la Materia CSIC, Madrid, Spain
8) Depart. Fis. Atomica Molecular Nuclear Universidad de Sevilla, and CNA, Sevilla, Spain
9) Departamento de Fısica Aplicada, Universidad de Huelva, Huelva, Spain
10) Department of Physics, Faculty of Science, University of Zagreb, Zagreb, Croatia
11) Division of Experimental Physics Ruder Boskovic Institute, Zagreb, Croatia

Spokespersons: A.Di Pietro, P.Figuera
Local contact name: M. Madurga

CERN-INTC-2016-018 / INTC-P-463
11/01/2016

Abstract

The aim of the proposed experiment is to investigate on the reaction dynamics of proton-halo induced collisions at energies around the Coulomb barrier where coupling to continuum effects are expected to be important. We propose to measure ^{8}B+^{64}Zn elastic scattering angular distribution together with the measurement, for the first time, of p-^{7}Be coincidences coming from transfer and/or break-up of ^{8}B. The latter will allow a better understanding of the relative contribution of elastic *vs* non-elastic break-up in reactions induced by extremely weakly-bound nuclei. We believe that with the availability of the post accelerated ^{8}B beam at REX-ISOLDE we will be able to collect for the first time high quality data for the study of such an important topic.

Requested shifts: [29] shifts
Beamline: 2nd beamline HIE-Isolde

1. **Physics case**

1.1 Evidences of ^{8}B p-halo structure

^{8}B is a drip line nucleus. With its very low threshold of 0.138 MeV against ^{8}B→^{7}Be+p break-up it is a good candidate for having a p-halo structure. The existence of a p-halo in ^{8}B has been debated in the literature. The interaction cross-section measured at energies larger than 100 A MeV did not show

enhancement with respect to the systematic of stable nuclei (see e.g. [(1), (2)]) and therefore a regular size of ^{8}B was initially deduced. A re-analysis performed by Al-Khalili and Tostevin [(3)] of the high-energy data [(1)], suggested that the previously assigned r.m.s. radius should be re-assigned, indicating a large extension of the last proton distribution beyond the core. At lower energies large enhancements of the interaction cross-section have been deduced from experimental data (see [(4), (5)]). A narrow momentum distribution of ^{7}Be is observed in ^{8}B break-up experiments performed at various energies and on several targets; the momentum distribution is however influenced by the reaction mechanism so it does not necessarily reflect the characteristics of the valence proton wave function [(6)]. A long tail of the density distribution is deduced from the reaction cross section analysis in [(4)] indicating the existence of the halo whereas in [(7)] a weakly developed p-halo is claimed. A large 1p-removal cross-section is found in [(4) (8) (9)] which accounts for the difference between interaction cross-sections of ^{8}B and ^{7}Be [(4)]. This behavior indicates a p+^{7}Be configuration in the wave function of ^{8}B with a proton decoupled from the other nucleons thus supporting the p-halo existence in ^{8}B.
In summary, most of the existing results are in favor of a p-halo configuration of ^{8}B. Due to the presence of the Coulomb barrier, which inhibits the occurrence of a halo in p-rich nuclei, ^{8}B is probably the only nucleus having a p-halo configuration in its ground state.

1.2 n-halo *vs* p-halo reactions

Huge efforts have been made in the past years to understand the reaction dynamics around the Coulomb barrier with n-halo nuclei. On the other hand the dynamics at the barrier with p-halo is expected to be different, but almost no experimental data exist [for a review see (10)].

Many of the investigations performed with ^{8}B beams concern Coulomb dissociation at energies well above the Coulomb barrier in order to get indirect information on the radioactive capture reaction ^{7}Be(p,γ) [(11)], but very little studies exist to investigate the reaction dynamics of p-halo nuclei. All experiments have been done using in-flight produced ^{8}B beam, therefore with the intrinsic limitations associated with the quality of such beams (purity, energy spread and beam emittance) compared to the post-accelerated ones. Coulomb dissociation of p-halo nuclei shows a different behaviour from n-halo, in fact, the loosely bound valence proton actively participates in the reaction process. Due to a dynamic polarization effect, the valence proton is expected to be displaced behind the nuclear core and shielded from the target; this effect causes a reduction of break-up probability compared to first-order perturbation theory predictions and higher-order corrections are required [e.g. (12) (13)]. As discussed in [(14)] nuclear processes are expected to have a primary role in the dissociation of ^{8}B. This has been experimentally observed in e.g. ^{8}B+^{208}Pb at 142 A MeV where it was found that the nuclear break-up accounts for about half of the total break-up cross-section [(2)]. Conversely for the n-halo nucleus ^{11}Be on the same target at a similar energy the Coulomb contribution far exceeds the nuclear one [(15)]. Contrary to the n-halo, in the case of p-halo the Coulomb interaction acts not only between the core and the target but also between the p and the core and the p and the target. In [(15)] the role of the p–core and p-target interaction in the p-halo break-up was studied theoretically. The effect of these additional potentials is to create an effective barrier, which makes the proton of the halo effectively more bound. This behavior could explain the apparent discrepancy in the interpretation of the different experiments, discussed in section 1.1, in terms of halo structure of ^{8}B. In this respect an interesting observable to measure is the p-breakup angular distribution. According to [(16) (17)] the nuclear breakup mechanism will give a relatively flat distribution, while the Coulomb breakup will be forward peaked.

At low energies, close to the Coulomb barrier, coupling effects dominate the dynamics. Since the ground state of halo nuclei lies very close to the continuum, coupling to the continuum affects the various processes. As a result of this coupling low energy elastic scattering angular distribution of n-

halo nuclei shows a suppression in the Coulomb-nuclear interference region [e.g. (18) (19) (20) (21) (22)]. A large total reaction cross-section is, as a consequence, observed. These results on heavy targets are due mainly to the coupling with the low-lying E1 strength in the continuum [(18) (20)], however in the case of our ^{11}Be+^{64}Zn experiment performed at Rex-ISOLDE on a medium mass target [(19)], nuclear as well as Coulomb coupling effects are important. For n-halo reactions a large fraction of total reaction cross-section is due to direct processes such as break-up or transfer [(22) (23) (24) (25)].

The elastic scattering ^{8}B+^{208}Pb at 170 MeV, well above the barrier, was recently measured in [(26)] using an in-flight ^{8}B beam having an intensity of $\approx 10^{2}$ pps. A Continuum Discretised Coupled Channel (CDCC) analysis of the angular distribution showed no effect of coupling to the continuum contrary to what is observed in the n-halo case. At the barrier, the ^{8}B elastic scattering and break-up on a ^{58}Ni target was measured [(5) (27) (28)] using the in-flight separated "cocktail" ^{8}B, ^{7}Be, ^{6}Li beam produced at the TwinSOL facility of Notre Dame. Due to the quality of the beam, the angular distributions were obtained for a limited number of angles and with a poor angular resolution. Unlike the ^{8}B+^{208}Pb result, the total reaction cross-section for ^{8}B+^{58}Ni was found to be large, as in the case of n-halo reactions. We would like to underline that our results on ^{11}Be+^{64}Zn [(19)] have shown that only if precise measurements are performed one can observe effects of the nuclear structure on the elastic scattering angular distribution. It was, in fact, possible to observe the peculiar shape of the ^{11}Be+^{64}Zn elastic angular distribution thanks to the high angular resolution of the measurement. In fact, in [(29)], we have demonstrated that the measured mean value of a rapidly varying function (i.e. the elastic scattering angular distribution in the present case), plotted versus the mean value of the variable (i.e. angle) is not representative of the function if the function is averaged over a large interval. Therefore, precise measurements are needed to extract reliably information on the reaction dynamics from the elastic scattering measurements.

For the ^{8}B+^{58}Ni the inclusive break-up was also measured [(27) (28)]; in order to describe the ^{7}Be break-up angular distribution, CDCC calculations, which considered an extended p-halo structure of ^{8}B, were performed. Coulomb-nuclear interference effects were found to be important even at very large distances. In this work, however, it was not possible to separate the contribution of transfer and break-up since inclusive data were measured.

For ^{8}B+^{58}Ni the fusion excitation function around the barrier was also deduced from the measured proton yield [(30)] and a large enhancement with respect to the n-halo case was found. A different result was obtained for ^{8}B+^{28}Si, where fusion cross-sections were deduced from the alpha yield and found similar to the n-halo nuclei case [(31)].

In summary, from reaction studies of p-halo nuclei a clear picture is not emerging. The availability of the post-accelerated ^{8}B beam of ISOLDE will offer a unique opportunity to shed some light on this topic.

2. Proposed experiment

The successful ^{9,10,11}Be+^{64}Zn experiment that we performed at Rex-Isolde (with a mean intensity of $7\text{x}10^{3}$ pps for ^{11}Be) and LNS (with ^{9}Be) [(19)], evidenced how low energy reactions are sensitive to the structure of the colliding nuclei.

In order to investigate further the reaction dynamics of p-halo nuclei, we propose to perform the measurement of a high-resolution elastic scattering angular distribution of the ^{8}B+^{64}Zn in the angular range $10° \leq \theta_{c.m.} \leq 100°$, deduce the total reaction cross-section and measure transfer and break-up. The measurements will be done at $E_{lab} \approx 4.5$ MeV/u in order to have an $E_{c.m.}/V_C$ similar to the one of the ^{11}Be experiment [(19)]. To the same aim we propose to measure for the first time also ^{7}Be-proton coincidences. In the present case, as in the ^{11}Be experiment, we propose to measure the reaction

induced by the weakly bound ^{7}Be, core of ^{8}B, on the same target. From the optical model (OM) analysis of these scattering data, the core-target potential can be extracted, this is a very important ingredient for the theoretical analysis of the ^{8}B data.

By measuring elastic scattering, break-up and transfer angular distributions one can pin-down information on the role of the nuclear and Coulomb contribution to the ^{8}B dissociation. In [(27)] the ^{7}Be angular distribution from the ^{8}B break-up showed that Coulomb-nuclear interference was acting at very large distance. In the same way, the observed damping of the Coulomb-nuclear interference peak in the elastic scattering angular distribution, particularly evident in the ^{11}Be+^{64}Zn case, originated by nuclear coupling occurring at large impact parameters due to the ^{11}Be halo structure. The OM analysis of the ^{11}Be+^{64}Zn elastic data showed that a very large surface diffuseness parameter (a_{si}=3.5 fm) is needed in order to reproduce the behavior of the cross-section in the region around the Coulomb-nuclear interference. This large diffuseness is related to the decay length of the neutron initial state wave function inside the halo nucleus [(32)]. Since elastic scattering is a peripheral process, it probes the wave function tail. Therefore, information on the halo structure can be directly inferred from elastic scattering measurement if detailed and high-resolution angular distributions are measured.

In figure 1 a preliminary CDCC calculation for the ^{8}B+^{64}Zn is shown together with the no-continuum coupling calculation. As one can see from the figure a reduction of the Coulomb-nuclear interference peak is predicted, although not as large as for the ^{11}Be case. In the figure the OM calculation of ^{7}B+^{64}Zn is shown, performed using a ^{7}Li+^{64}Zn potential from the literature. The OM potential used for this calculation was used as a bare potential for the CDCC calculation of ^{8}B scattering.

The aim of the present proposal, as mentioned above, in addition to the measurement of elastic scattering and total reaction cross-section of ^{8}B+^{64}Zn, is to obtain information on the relative contribution of transfer and break-up cross-sections. This is very important, and it is done for the first time for low energy ^{8}B reaction. Note that the in ^{8}B+^{58}Ni [(27)] inclusive break-up was measured,

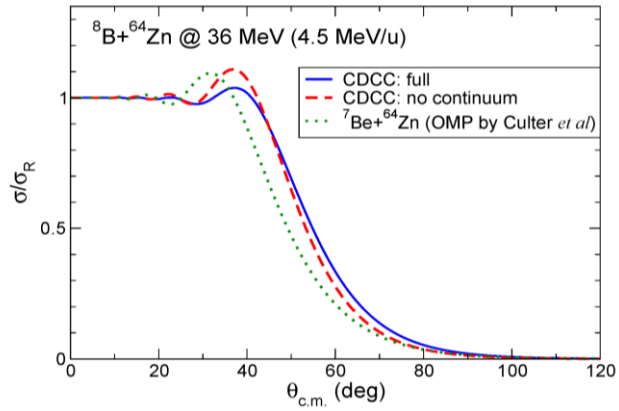

Figure 1. Calculated elastic scattering angular distribution. (Dotted) ^{7}Be+^{64}Zn optical model calculation. (Dashed) ^{8}B+^{64}Zn CDCC calculation without continuum coupling. (Full line) ^{8}B+^{64}Zn CDCC calculation with continuum coupling. See text for details.

where the proton removed from ^{7}Be can be either scattered or absorbed. The present experiment allows to determine, on top of the inclusive break-up, the clean, exclusive break-up. From the analysis of the p-^{7}Be coincidences, one can determine the energy distribution of the proton with respect to the ^{7}Be fragment and separate the contribution of the different direct processes. A signal of the halo character of ^{8}B will be that a sizeable fraction of the break-up cross section will correspond to final states in which the relative energy of protons and ^{7}Be will be small, so that protons and ^{7}Be come out at similar

scattering angles. In the case of transfer, in fact, based on energy-momentum matching considerations, the p-transfer will preferably occur to highly excited states of the residual nucleus ^{65}Ga (Q_{opt}=-3.5 MeV, E_x=18.8 MeV). Consequently, transfer to the bound state of ^{65}Ga (Q_{gg}=3.8 MeV) is expected to be very small. In ^{8}B+^{58}Ni [(27)] the inclusive–break-up measured was consisting mainly of elastic breakup (i.e. breakup without proton absorption and without target excitation). This is in contrast to what found in other situations (for example, in ^{6}Li reactions most of the inclusive alpha cross section seems to come from non-elastic breakup) [(33)].

We performed Montecarlo simulations of the energy spectrum of ^{7}Be and p coming from break-up processes. With the experimental set-up proposed in the following, the efficiency to detect ^{7}Be-p coincidences coming from break-up is about 70%. This value takes into consideration the detection thresholds.

3. Experimental set-up.

The proposed experimental set-up is similar to the one used for the ^{11}Be+^{64}Zn IS438 experiment [(19)] and it is shown in figure 2. The choice of ^{64}Zn as a target is due to the fact that on this target we have measured elastic scattering and reactions with halo (^{6}He,^{11}Be) (^{11}Li experiment has been approved by the EEC of TRIUMF) and weakly-bound beams (^{6,7}Li,^{9}Be), so we have already a wide systematic.

A target of 1mg/cm^2 will be surrounded by four Si detector telescopes. Each telescope will be composed by a 40 μm ΔE Si strip detector (50×50 mm^2 divided into 16+16 strips) and 1000 μm residual energy DSSSD detector (50×50 mm^2 divided into 16+16 strips). With this set-up the angular range $10°\leq\theta_{c.m.}\leq100°$ can be covered, and it will be possible to charge identify the scattered ^{8}B and the break-up fragments ^{7}Be and ^{1}H.

The target will be tilted at ≈25° with respect to the beam axis in order to allow measuring also at angles around 90°.

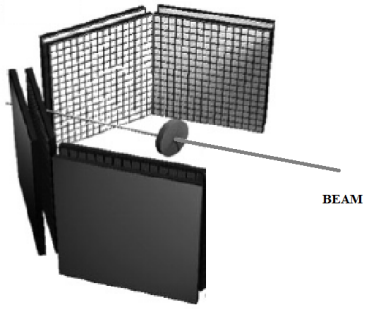

Figure 2. Sketch of the experimental set-up

4. Estimate of beam time request.

For the estimate of beam time we assumed an average ^{8}B intensity of 5×10^3 pps. With the proposed geometry we will be able to measure in 21 shifts the angular distribution at two degree step up to $\theta_{c.m.}$≈40° (Coulomb-nuclear interference region) with a statistical error < 3% sufficient to observe the effect predicted by the CDCC calculations. An angular step of 3° and 4° will be used for the angles larger than 40° depending upon the angle and the corresponding predicted statistics. Concerning the ^{7}Be-p coincidences, it has been estimated that in the requested BTU, a total of ≈500 coincidences will be collected. ^{7}Be-p break-up events will be concentrated in the forward detector, allowing the

measurement of the angular distribution.
The ^{7}Be+^{64}Zn elastic scattering will be measured as well, in order to get information on the core-target optical potentials. According to the production yield available on the Isolde web, ^{7}Be should have a intensity similar to the ^{10}Be beam, i.e. 10^{7} pps on the target of the experiment, intensity that was achieved in our previous ^{10}Be experiment [(19)]. We ask for 4 shifts for the ^{7}Be+^{64}Zn experiment (E_{lab}=4.5 MeV/u) to collect enough statistics at large angles in the elastic scattering. For the ^{8}B+^{64}Zn we ask for a total of 21 shifts at E_{lab}=4.5 MeV/u. In addition we ask for 4 shifts for stable beam adjustments, calibrations and beam changing at REX-ISOLDE. A total of 29 shifts are requested.

6. References

1. I.Tanihata. s.l. : Phys.Lett. B, 1988, Vol. 206, p. 592.
2. B. Blank et al. s.l. : Nucl. Phys. A, 1997, Vol. 624, p. 242.
3. J.S. Al-Khalili and J.A. Tostevin,. s.l. : Phys. Rev. Lett., 1996, Vol. 76, p. 3903 .
4. M. Fukuda et al. s.l. : Nucl. Phys. A, 1999, Vol. 656, p. 209.
5. E.F. Aguleira et al. s.l. : Phys. Rev. C, 2009, Vol. 79, p. 021601(R).
6. J.H. Kelley et al. s.l. : Phys. Rev. Lett., 1996, Vol. 76, p. 3903.
7. F. Negoita et al. s.l. : Phys. Rev. C, 1996, Vol. 54, p. 1787.
8. W. Schwabet al. s.l. : Z.Phys. A, 1995, Vol. 350, p. 283.
9. M.H. Smedberg et al. s.l. : Phys. Lett. B, 1999, Vol. 452, p. 1.
10. L.F.Canto et al. s.l. : Phys. Rep., 2015, Vol. 596, p. 1.
11. B. Davidset et al. s.l. : Phys. Rev. C, 2001, Vol. 63, p. 065806. and ref. therein.
12. A. Garcìa-Camacho et al. s.l. : Phys. Rev. C, 2007, Vol. 76, p. 014607.
13. J.F. Liang et al. s.l. : Phys. Lett. B, 2009, Vol. 681, p. 22.
14. C. Dasso et al. s.l. : Nucl. Phys. A, 1998, Vol. 639, p. 635.
15. A. Bonaccorso et al. s.l. : Phys. Rev. C, 2004, Vol. 69, p. 024615 .
16. J. Margueron et al. s.l. : Nucl. Phys. A, 2002, Vol. 703, p. 105.
17. R. Kumar and A.Bonaccorso. s.l. : Phys. Rev. C, 2011, Vol. 84, p. 014613.
18. A.M. Sanchez-Benitez et al. s.l. : Nucl. Phys. A, 2008, Vol. 803, p. 30.
19. A. Di Pietro et al. s.l. : Phys. Rev. Lett., 2010, Vol. 105, p. 022701.
20. M. Cubero et al. s.l. : Phys.Rev.Lett., 2012, Vol. 109, p. 262701 .
21. A. Di Pietro et al. s.l. : Phys. Rev. C, 2012, Vol. 85, p. 054607.
22. A. Di Pietro et al. s.l. : Phys.Rev. C, 2004, Vol. 69, p. 044613.
23. E.F. Aguilera et al. s.l. : Phys Rev. C, 2001, Vol. 63, p. 061603.
24. R. Raabe et al. s.l. : Nature, 2004, Vol. 431, p. 823.
25. J.P.Fernandez-Garcia et al. s.l. : Phys.Rev.Lett., 2013, Vol. 110, p. 142701.
26. Y.Y. Yang et al. s.l. : Phys. Rev. C, 2013, Vol. 87, p. 044613.
27. V. Guimaraes et al. s.l. : Phys. Rev. Lett., 2000, Vol. 84, p. 1862.
28. J.J. Kolata et al. s.l. : Phys Rev. C, 2001, Vol. 63, p. 024616.
29. M. Fisichella et al. s.l. : Phys. Rev. C, 2015. p. 064611. Vol. 92.
30. E.F. Aguilera et al. s.l. : Phys. Rev. Lett, 2011, Vol. 107, p. 092701.
31. A. Pakou et al. s.l. : Phys. Rev. C, 2013, Vol. 87, p. 014619.
32. A. Bonaccorso and F. Carstoiu. s.l. : Nucl. Phys. A, 2002, Vol. 706, p. 322.
33. Jin Lei and A. M. Moro. s.l. : Phys. Rev. C, 2015, Vol. 92, p. 044616 .
34. N. Keeley et al. s.l. : Prog. Part. Nucl. Phys, 2009, Vol. 63, p. 396.

Appendix

1 DESCRIPTION OF THE PROPOSED EXPERIMENT

The experimental setup comprises: *(name the fixed-ISOLDE installations, as well as flexible elements of the experiment)*

Part of the Choose an item.	Availability	Design and manufacturing
[if relevant, name fixed ISOLDE installation: MINIBALL + only CD, MINIBALL + T-REX]	☐ Existing	☐ To be used without any modification
[Part 1 of experiment/ equipment]	☒ Existing	☐ To be used without any modification ☐ To be modified
	☐ New	☒ Standard equipment supplied by a manufacturer ☐ CERN/collaboration responsible for the design and/or manufacturing
[Part 2 experiment/ equipment]	☐ Existing	☐ To be used without any modification ☐ To be modified
	☐ New	☐ Standard equipment supplied by a manufacturer ☐ CERN/collaboration responsible for the design and/or manufacturing
[insert lines if needed]		

2

3 HAZARDS GENERATED BY THE EXPERIMENT

(if using fixed installation) Hazards named in the document relevant for the fixed [MINIBALL + only CD, MINIBALL + T-REX] installation.

Additional hazards:

Hazards	*[Part 1 of the experiment/equipment]*	*[Part 2 of the experiment/equipment]*	*[Part 3 of the experiment/equipment]*
Thermodynamic and fluidic			
Pressure	[pressure][Bar], [volume][l]		
Vacuum	Interlocked beamline valve to LINAC		
Temperature	[temperature] [K]		
Heat transfer			
Thermal properties of materials			
Cryogenic fluid	[fluid], [pressure][Bar], [volume][l]		
Electrical and electromagnetic			
Electricity	[voltage] [V], [current][A] ±12V, ±24V DC power 300 V Si detectors		
Static electricity			
Magnetic field	[magnetic field] [T]		

Batteries	☐		
Capacitors	☐		
Ionizing radiation			
Target material	[material]		
Beam particle type (e, p, ions, etc)	8B, 7Be, 12C		
Beam intensity	10^3-10^7 pps		
Beam energy	4.5 MeV/u		
Cooling liquids	[liquid]		
Gases	[gas]		
Calibration sources:	☒		
• Open source	☒ alpha sources		
• Sealed source	☐ [ISO standard]		
• Isotope	Gd, Am, Pu,Cm		
• Activity	≈1kBq		
Use of activated material:			
• Description	☐		
• Dose rate on contact and in 10 cm distance	[dose][mSV]		
• Isotope			
• Activity			
Non-ionizing radiation			
Laser			
UV light			
Microwaves (300MHz-30 GHz)			
Radiofrequency (1-300MHz)			
Chemical			
Toxic	[chemical agent], [quantity]		
Harmful	[chemical agent], [quantity]		
CMR (carcinogens, mutagens and substances toxic to reproduction)	[chemical agent], [quantity]		
Corrosive	[chemical agent], [quantity]		
Irritant	[chemical agent], [quantity]		
Flammable	[chemical agent], [quantity]		
Oxidizing	[chemical agent], [quantity]		
Explosiveness	[chemical agent], [quantity]		
Asphyxiant	[chemical agent], [quantity]		
Dangerous for the environment	[chemical agent], [quantity]		
Mechanical			
Physical impact or mechanical energy (moving parts)	[location]		
Mechanical properties (Sharp, rough, slippery)	[location]		
Vibration	[location]		
Vehicles and Means of Transport	[location]		
Noise			
Frequency	[frequency],[Hz]		
Intensity			
Physical			
Confined spaces	[location]		

High workplaces	[location]		
Access to high workplaces	[location]		
Obstructions in passageways	[location]		
Manual handling	[location]		
Poor ergonomics	[location]		

0. Hazard identification

3.2 Average electrical power requirements (excluding fixed ISOLDE-installation mentioned above): *(make a rough estimate of the total power consumption of the additional equipment used in the experiment)*: *15 kW*